PCCP



View Article Online **PAPER**



Cite this: Phys. Chem. Chem. Phys., 2025, 27, 7258

Received 24th December 2024. Accepted 17th March 2025

DOI: 10.1039/d4cp04843a

rsc.li/pccp

On the relation of structure and dynamics in aromatic ring-tail structured liquids†

Rolf Zeißler, * Jan Philipp Gabriel. Dorthe Posselt * and Thomas Blochowicz

We present a combined X-ray and depolarized dynamic light scattering study on a series of liquid phenylalkanes, consisting of an aromatic phenyl ring attached to an alkyl chain of varying length. We study the influence of competing interactions of rings and chains on liquid structure and molecular reorientation. The X-ray scattering curves of the investigated liquids show a weak prepeak in a q range below the main scattering peak, indicating a certain degree of structure formation on a larger length scale than commonly found in simple liquids. As a function of temperature and alkyl chain length, we find that the observed prepeak shares some characteristics with that found for ionic liquids, suggesting a similar origin, i.e., domains of ring groups separated by alkyl chains leading to nanometer-scale structuring. Furthermore, with increasing chain length, the scattering curves show a distinct transition in the temperature dependence of the prepeak amplitude, which is mirrored in the activation energy of molecular reorientation, obtained via depolarized dynamic light scattering. As a possible interpretation, we suggest that ring-ring interactions control structure as well as dynamics for short alkyl chains but rapidly lose influence above a certain alkyl chain length. Since phenylalkanes are among the most simple representatives of liquids consisting of aromatic and non-aromatic units, we regard this work as a proof of concept to study the coupling of structure and dynamics in liquids with competing interactions weaker than both Coulombic interactions and hydrogen bonding.

1. Introduction

Formation of supramolecular structures is very common in bulk liquids with competing interactions. Examples include the formation of domains with different polarity in ionic liquids, 1,2 or the formation of supramolecular structures in hydrogen bonding systems, with monohydroxy alcohols being a prominent example.³ Often such structure formation has a clear impact on the dynamics, where, e.g., an additional Debye-like process is observed in the dielectric loss of monoalcohols^{4,5} or, similarly, a slow relaxation mode in ionic liquids, ^{6,7} both of which are argued to result from supramolecular structure formation. However, most of the existing studies investigating the interplay between structure and dynamics focus on liquids of molecules with strongly competing interactions, such as hydrophillic/hydrophobic or polar/apolar molecular components, where the origin of the resulting supramolecular structures is the built-in frustration.

Things are much less clear, however, when such stronger opposing interactions are absent and weaker interactions become dominant in determining liquid structuring.

In order to investigate the complex interplay of structure and dynamics in liquids, frequently combinations of scattering methods and dynamic measurement techniques are used, often with the aim of identifying dynamic peculiarities that are believed to be connected to specific structural features. For this purpose, it has proven successful to compare temperature and/or pressure dependent data obtained by the different methods, as well as to systematically vary the chemical composition of the liquids under study. 8-10 The present study pursues a very similar goal, using X-ray scattering and depolarized dynamic light scattering to investigate the interplay between liquid structure and dynamics in a series of 1-phenylalkanes, which consist of an alkyl chain of varying length attached to an aromatic phenyl ring, representing the class of aromatic ringtail structured liquids.

In the current study we demonstrate that both structure and dynamics of a series of 1-phenylalkanes show a distinct transition at a certain alkyl chain length. As a possible mechanism underlying this change, we suggest that structure and dynamics is dominated by interaction of the aromatic ring groups below a certain alkyl chain length while the alkyl chains dominate the behavior above a certain chain length. As the source of this

^a Institute for Condensed Matter Physics, Technical University of Darmstadt, Germany. E-mail: rolf.zeissler@pkm.tu-darmstadt.de

^b Institute of Materials Physics in Space, German Aerospace Center, 55170 Cologne, Germany

^c IMFUFA, Centre for Frustrated Molecular Interactions, Department of Science and Environment, Roskilde University, Denmark

[†] Electronic supplementary information (ESI) available. See DOI: https://doi.org/ 10.1039/d4cp04843a

transition we point to a competition of the interactions between the aromatic rings and the interactions between the alkyl chains. Such an interplay of interactions may be essential for local structuring and the dynamic behavior of many liquids, where stronger effects of dipolar interactions or hydrogen bonding are absent.

2. Experimental details

Table 1 shows the investigated liquids with abbreviations, suppliers, chemical purity, melting points and investigated temperature ranges. The abbreviations were chosen in accordance with our previous study. 11 Pn is an abbreviation referring to the 1-phenylalkanes where n is the number of carbon atoms in the alkyl chain. Cn is an abbreviation referring to the corresponding *n*-alkanes.

WAXS and SAXS were performed at RUCSAXS, Roskilde University Interdisciplinary X-ray scattering Hub, on a Xenocs Xeuss 3.0 UHR XL instrument equipped with an Eiger 2R 1 M detector from Dectris. The source is a Xenocs GeniX 3D Cu- K_{α} (wavelength $\lambda = 1.5406 \text{ Å}$) HFVL X-ray tube with focusing optics. The liquids to be investigated are filled into 80 mm long borosilicate capillary tubes from Hilgenberg with an outer diameter of 1.5 mm. The capillaries are then sealed by an epoxy-based two-component glue. P19 had to be melted at 90 °C before it could be filled into the capillary tube. During X-ray measurements the sample tubes were inserted into the heating block of a HFSX350-CAP stage by LINKAM, which can vary the temperature in a range of approximately 80 K to 620 K, according to the manufacturer. Temperature stabilization occurs via an interplay of liquid nitrogen flow and control of the heating power of the heating block. The temperatures given throughout are the set temperatures of the Linkam stage. The measurements are performed under vacuum and calibration shows that the absolute sample temperature is highly dependent on the pressure in the sample chamber and shows only limited reproducibility when a cuvette is reinserted into the Linkam stage due to the capillary having only few random close contact points with the stage. However, for each liquid measured, the capillary was not removed from the stage during measurements. We also note that none of the conclusions drawn from the X-ray data in this work rely on high accuracy of the sample temperatures. Measurements were performed at three different sample-detector distances, i.e. 90 m, 300 m and 1800 m

to obtain the scattering intensity in a q-range of approximately 0.02 Å^{-1} to 2.5 Å^{-1} . The lower bounds of the investigated temperature ranges were set by the melting points of the liquids and the upper bounds were chosen to approximately match those of the dynamic measurements in ref. 11. Additional room temperature measurements were performed for each liquid with a sample-detector distance of 42.5 mm thus extending the high end of the q-range to 3.74 \mathring{A}^{-1} . For all scattering curves presented in this work a background contribution was subtracted, which was determined by measuring the intensity scattered from an empty capillary at the same sample detector distances and acquisition times. The most prominent contribution to the X-ray scattering curves I(q), *i.e.*, the scattered intensity as a function of the absolute value of the scattering vector $q = \frac{4\pi}{\lambda}\sin(\theta/2)$, where λ is the X-ray wavelength and θ is the scattering angle, is the main scattering peak, which is usually assigned to nearest-neighbour intermolecular spatial correlations. 12 For some systems, this main scattering peak is accompanied by weaker features, e.g. a peak in the q range below the main peak arising from spatial correlations on length scales larger than the average distance between neighbouring molecules. These prepeaks have been observed for various molecular liquids, e.g., ionic liquids, 13-15 alcohols 16-18 and liquids of amphiphilic molecules 19-23 and are usually associated with some form of supramolecular structure formation.

Depolarized dynamic light scattering (DDLS) spectra were obtained via tandem Fabry-Perot interferometry employing a scanning multipass tandem Fabry-Perot interferometer (TFPI) by IRS Scientific Instruments. In the experiment the sample is contained in a cuvette, which is placed in an oven for measurements above room temperature or an optical cryostat for measurements below room temperature. For the oven temperature accuracy is approximately 2 K and for the cryostat 0.5 K. The sample is impinged by the beam of a Coherent Verdi V2 laser with a wavelength of 532 nm and the spectral density $I(\nu)$ of the depolarized component of the light scattered from the sample is measured by the TFPI in backscattering geometry. The imaginary part of the DDLS susceptibility $\gamma''(\nu)$ is then calculated via the fluctuation dissipation theorem

$$\chi''(\nu) = \frac{I(\nu)}{n(\nu, T) + 1}$$
 (1)

where $n(\nu,T) = (\exp(h\nu/k_BT) - 1)^{-1}$ is the Bose temperature factor. At this point it should be emphasized that in a DDLS

Table 1 Table of investigated substances

Substance	Abbreviation	Supplier	Chemical purity (%)	$T_{\rm m}$ (K)	T _{SAXS/WAXS} (K)	$T_{ m DDLS}$ (K)
Toluene		Acros Organics	99.8	178		210-270
<i>n</i> -pentane	C5	Thermo Scientific	>99	143		180-240
<i>n</i> -octane	C8	Acros Organics	>98	216		295-360
<i>n</i> -tridecane	C13	Alfa Aesar	>98	268		320-380
<i>n</i> -nonadecane	C19	TCI	>98	305		390-450
1-phenylbutane	P4	Thermo Scientific	>99	185	200-380	240-300
1-phenylhexane	P6	Thermo Scientific	>99	212		280-380
1-phenyloctane	P8	Acros Organics	>99	237	240-420	300-420
1-phenyltridecane	P13	TCI	>99	283	290-420	320-420
1-phenylnonadecane	P19	TCI	>98	308	320-500	400-500

experiment the reorientation dynamics of molecules is probed, independent of the wavelength and scattering angle.^{24,25} The most prominent feature of the DDLS spectra is the structural relaxation peak, the position and shape of which provides information on the distribution of molecular reorientation times.26,27 For more details on the experimental setup the reader is referred to ref. 11 and 25. The DDLS data of P8, P13 and P19 have been previously published in ref. 11. The investigated temperature ranges are shown in Table 1.

3. Results

3.1. Structure

Fig. 1 shows the X-ray scattering curves at the lower limit of the respective investigated temperature ranges (see Table 1) for four 1-phenylalkanes with chain lengths varying from n = 4 to n = 19. There are two clear peak-like features in the scattering curves that are marked by arrows in part (a) of the figure: the main scattering peak at $q \simeq 1.4 \text{ Å}^{-1}$ for all samples and a prepeak with varying position in the range 0.2 $\mathring{A}^{-1} \leq q \leq$ 0.9 Å^{-1} . The position of the prepeak systematically shifts to lower q with increasing chain length. Part (b) of Fig. 1 shows the

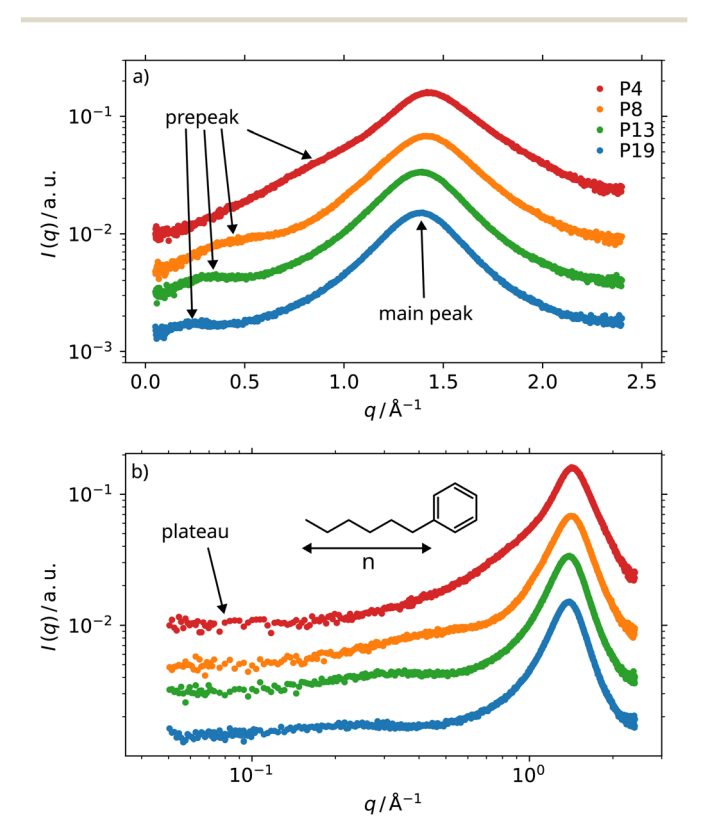


Fig. 1 (a) Scattering curves of 1-phenylalkanes with varying chain lengths at the lower bound of the respective investigated temperature ranges (increasing chain length from top to bottom) shifted in amplitude for comparison. The arrows mark the two immediately visible features of the spectra, the main scattering peak at $q \simeq 1.4 \, {\rm \AA}^{-1}$ and a prepeak at $0.2 \, {\rm \AA}^{-1} \le$ $q \le 0.9 \text{ Å}^{-1}$. The position of the prepeak shifts to lower q with increasing chain length. (b) Data of (a) plotted with a logarithmic q-axis revealing an additional plateau-like feature at $q \lesssim 0.1 \, \text{Å}^{-1}$. The structural formula of the molecules under study is also shown in the figure.

same set of data on a logarithmic q-axis, revealing an additional plateau-like feature, i.e. approximately q-independent scattering at $q \lesssim 0.1 \text{ Å}^{-1}$. To gain an understanding of the origin of the different contributions to the nanoscale structuring and the resulting X-ray scattering curves, a detailed investigation of the temperature and chain length dependence was performed.

Fig. 2(a) shows the scattering curve of P13 at room temperature, measured with the shortest sample detector distance, i.e., the q-range extending furthest up in q. Here an additional peak at $q \simeq 3 \text{ Å}^{-1}$, i.e., the high q side of the main peak is revealed. This type of peak is often assigned to intramolecular spatial correlations, 12,28 an interpretation we will follow in the analysis of our data. Thus, to shed light on the origin of the low q prepeaks in our system, temperature scans resolving the low-q regime were favored over resolving the intramolecular high q peak. The q-range was accordingly set to 0.02 $\mathring{A}^{-1} \leq q \leq$ 2.5 Å^{-1} . However, the information on the intramolecular peak gained from the room temperature WAXS measurements was used for the curve fitting of the scattering curves, i.e., the position and width of this peak were fixed for all other temperatures, since the peak is not expected to change much with temperature due to its intramolecular origin.

The colored curves in Fig. 2(a) represent model functions chosen to qualitatively describe the different contributions to the scattering curves. For the main scattering peak and the intramolecular peak, Lorentzian functions were chosen.

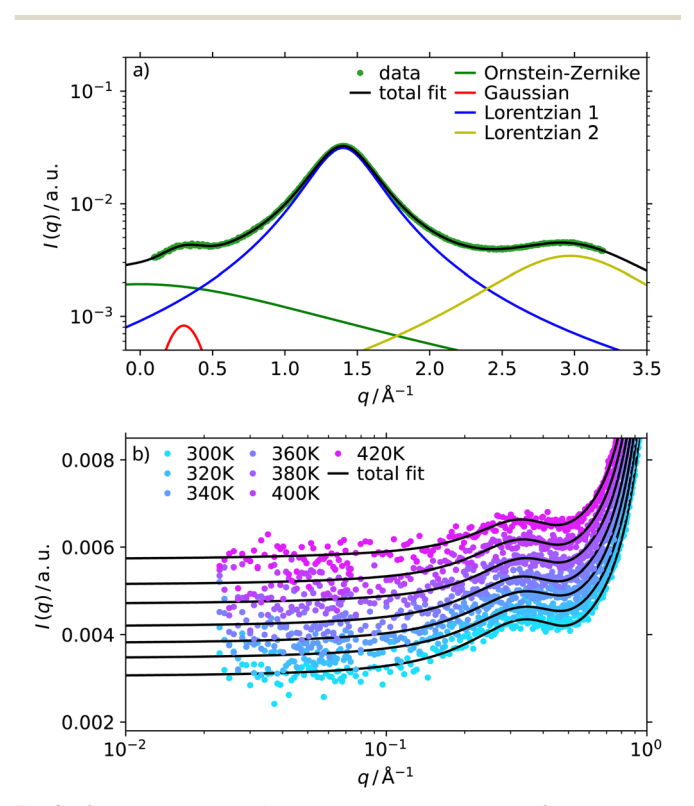


Fig. 2 Scattering curve of P13 at room temperature. Colored curves represent model functions describing the different contributions (see text) to the scattering curve and the black curve denotes the total fit function. (b) Scattering curves of P13 at $q < 1 \text{ Å}^{-1}$ for selected temperatures highlighting the good agreement of the data and the fit at low q.

The prepeak was described by a Gaussian function and the plateau at low q by an Ornstein-Zernike function

$$I_{\rm OZ}(q) = \frac{A_{\rm OZ}}{1 + (q\xi_{\rm OZ})^2}.$$
 (2)

This function takes on a constant value A_{OZ} for $q \rightarrow 0$ and decays on the characteristic length scale ξ_{OZ} . Part (b) of Fig. 2 shows the absolute scattering intensity of P13 at $q \leq 1 \text{ Å}^{-1}$ for selected set temperatures covering the whole temperature range. This comparison highlights the good agreement of the data and the fit at low q. The fit model was selected with reference to the literature and with the aim of minimizing the number of free fitting parameters. A more detailed description of the fit model including tables containing all parameters obtained with this model can be found in the ESI,† of this work. A comparison with standard small-angle scattering models, assuming a specific nanoscale structuring of rings in a matrix of alkyl chains, is also presented in the ESI,† but this approach does not overall lead to different conclusions for the present data sets.

Fig. 3(a) shows the temperature dependence of the prepeak position. Due to the small separation between the prepeak and the main scattering peak for P4, fitting with free parameters was not possible over the whole temperature range. Therefore, P4 was excluded from the analysis of the temperature dependence of the fitting parameters. For the other liquids, the curve fitting yields an approximately temperature independent position of the prepeak. In the inset, the corresponding length scale L \simeq $2\pi/q_{\rm peak}$ is shown for the four liquids. This length scale should be seen as an approximation of the average distance between the centers of regions with different electron densities, giving a rough idea of the possible origin of the prepeak, however, can not provide unambiguous information on the exact nature of structure formation. For $n \geq 8$ the prepeak position averaged over temperature was used and for P4 the position obtained from the room temperature measurement. The obtained length scales are ≈ 7 Å for P4, ≈ 14 Å; for P8, ≈ 21 Å; for P13 and \approx 28 Å; for P19. Especially for $n \ge 8$ these values exceed the length of a single molecule (≈ 8 Å; and ≈ 13 Å; for a stretched chain of eight and thirteen carbon atoms respectively³¹), ruling out a possible intramolecular origin of the prepeak. The black line in the insert indicates a linear dependence of the peak position on the length of the alkyl chain. A similar chain length dependence has been observed for imidazolium based ionic liquids and dialkyl carbonates in the literature, 1,23 where it was interpreted as indicative of aggregation of alkyl tails, thus separating domains of polar groups.

Fig. 3(b) shows the amplitude of the prepeak A_G for the four liquids. The results show that for P8 the amplitude is virtually temperature independent, whereas a noticeable decrease is observed for $n \geq 13$. A similar effect of the alkyl chain length on the temperature dependence of the amplitude of the prepeak has been reported for imidazolium based ionic liquids in the literature.³² The authors pointed out that this difference in temperature dependence could arise due to an increasing influence of alkyl chains on the structure formation.

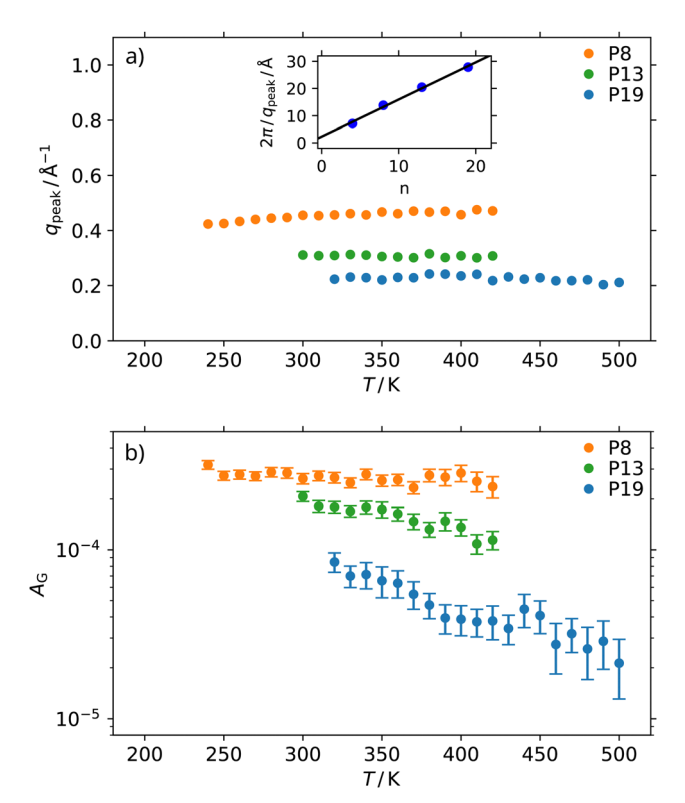


Fig. 3 (a) Position of the prepeak determined by fitting the model described in the text and in the ESI,† to the X-ray scattering curves as function of temperature. The inset shows the corresponding length scale $L = 2\pi/q_{peak}$ of the prepeak in dependence on the chain length (see text). (b) Amplitude of the Gaussian peak function describing the prepeak A_G . As function of temperature. Temperatures are relating to the sample stage temperature.

3.2. Dynamics

To relate the observed structural properties of the 1-phenylalkanes to their dynamics, the following section contains a detailed comparison of results from depolarized dynamic light scattering (DDLS) partially published in a previous work. 11

Fig. 4(a) shows DDLS spectra at different temperatures of the 1-phenylalkanes with varying chain length and of toluene, which represents the 1-phenylalkane of alkyl chain length n = 1, normalized to their maximum amplitude and rescaled to match the low frequency side of the P13 spectrum. This way of presentation was chosen to highlight differences in the spectral shape of the main relaxation peak between liquids analogous to the analysis in ref. 11. It should be noted that the figure only shows the section of the DDLS spectra containing the relaxation peak contribution, whereas the regime of vibrational contributions (~ 1 THz) is omitted for clarity in relation to the discussion in this paper. The temperatures chosen for this comparison were 210 K for toluene, 250 K for P4, 280 K for P6, 300 K for P8, 360 K for P13 and 420 K for P19. The temperatures were chosen in such a way that peak frequencies of the spectra are similar ($\nu_{\rm peak} \sim 1.5$ GHz). We emphasize that the observed differences between the spectra are not due to the different temperatures chosen for the comparison. The 1-phenylalkanes show a bimodal relaxation peak, which becomes more pronounced with increasing chain length, resulting

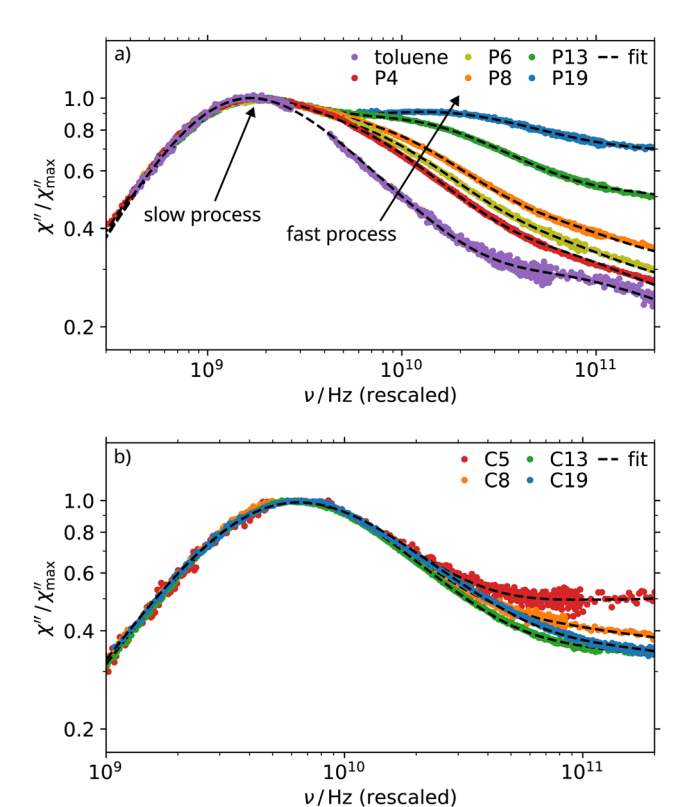


Fig. 4 (a) Depolarized dynamic light scattering (DDLS) spectra of the 1-phenylalkanes (toluene at 210 K, P4 at 250 K, P6 at 280 K, P8 at 300 K, P13 at 360 K and P19 at 420 K) rescaled with a prefactor to match the low frequency side of the spectrum of P13 and normalized to the maximum amplitude. The data of P8, P13 and P19 have previously been published in ref. 11. Temperatures for this comparison were chosen in such a way that peak relaxation times of the different spectra are similar ($\nu_{\rm peak} \sim$ 1.5 GHz). The spectra show bimodal relaxation peaks with an increasing separation between the two contributions with increasing chain length. The inset shows the correlation between the dynamic separation $\tau_{\text{slow}}/\tau_{\text{fast}}$ and the length scale corresponding to the position of the prepeak. (b) DDLS spectra of *n*-alkanes rescaled with a prefactor to match the low frequency side of the spectrum of C13 and normalized to the maximum amplitude (C5 at 180 K, C8 at 295 K, C13 at 380 K and C19 at 420 K). In the case of the n-alkanes the spectral shape of the relaxation peak is largely chain length independent in the considered chain length regime.

in two distinct contributions for $n \ge 8$ marked by arrows in Fig. 4(a). In ref. 11 which also considered aromatic ring-tail structured liquids with different ring groups, this bimodality of the relaxation peaks was shown to arise from dynamic decoupling of the ring group from the rest of the molecule. The fast contribution was assigned to rotation of the ring relative to the chain and the slow contribution to reorientation of the chain, or, respectively, the whole molecule. This interpretation is mainly based on the following observations: The separation of the two contributions increases with increasing length of the alkyl chain, the relative amplitude of the fast contribution is larger for rings with higher optical anisotropy and the bimodality shows up in dielectric loss spectra only if the ring contains a significant portion of the molecular dipole moment. The term dynamic decoupling was chosen since the two contributions have different temperature dependencies. As shown in ref. 11 this results in the spectra at different temperatures not collapsing onto a master curve, in contrast to liquids that do not show strong dynamic decoupling of different molecular units.33

Fig. 4(b) shows DDLS spectra of *n*-alkanes with varying chain length rescaled by a prefactor to match the low frequency side of the spectrum of C13 and normalized to the maximum amplitude. In contrast to the spectra of the 1-phenylalkanes, the relaxation peaks of the *n*-alkanes are monomodal in the investigated range of chain lengths. Furthermore, the spectral shape of the relaxation peaks is virtually independent of the chain length. This emphasizes again the strong influence of the dynamic decoupling on the DDLS spectra of 1-phenylalkanes.

Fig. 5(a) shows peak relaxation times for the slow contribution of the 1-phenylalkanes, attributed to the reorientation of the molecule as a whole, and peak relaxation times of the monomodal relaxation peaks of the *n*-alkanes and toluene. The peak relaxation times were obtained by the curve fitting approach presented in ref. 11. In this approach the bimodal relaxation peaks are described by a superposition of two Cole-Davidson functions

$$\chi''(\nu) = \Im \left\{ \frac{A_{\rm CD}}{(1 + i \cdot 2\pi\nu\tau_{\rm CD})^{\beta_{\rm CD}}} \right\},\tag{3}$$

where $\tau_{\rm CD}$ is the Cole–Davidson relaxation time, $\beta_{\rm CD}$ the Cole– Davidson stretching parameter and A_{CD} a constant. The stretching parameters are not analyzed in the current work, however,

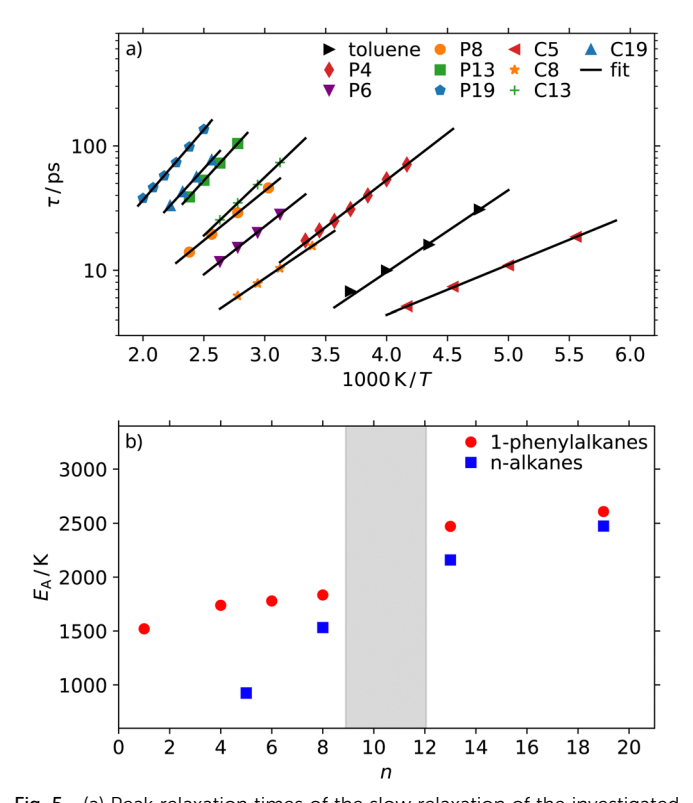


Fig. 5 (a) Peak relaxation times of the slow relaxation of the investigated 1-phenylalkanes and n-alkanes. Lines represent fits with the Arrhenius equation (eqn (4)). (b) Activation energies obtained from fitting eqn (4). The grey shaded area indicates the transition from ring dominated to chain dominated dynamics.

Paper

Table 2 Activation energies of molecular reorientation

Substance	Abbreviation	$E_{\mathrm{A}}\left(\mathrm{K}\right)$	
Toluene		1520(54)	
1-phenylbutane	P4	1738(28)	
1-phenylhexane	P6	1779(25)	
1-phenyloctane	P8	1834(8)	
1-phenyltridecane	P13	2471(19)	
1-phenylnonadecane	P19	2609(38)	
<i>n</i> -pentane	C5	926(13)	
<i>n</i> -octane	C8	1532(21)	
<i>n</i> -tridecane	C13	2159(24)	
<i>n</i> -nonadecane	C19	2474(14)	

the reader is referred to ref. 11 for some values. Peak relaxation times can be calculated as $\tau_{\rm peak} = \tau_{\rm CD} \cdot \tan^{-1}(\pi/(2\beta_{\rm CD} + 2))$. The lines in Fig. 5 represent fits of the peak relaxation times with the Arrhenius equation:

$$\tau(T) = a \cdot e^{E_A/T},\tag{4}$$

where E_A is the activation energy in units of Kelvin and a is a prefactor. Structural relaxation in molecular liquids usually only shows an Arrhenius temperature dependence far above the glass transition temperature and the onset of this behaviour depends on the liquid under study.35 Some of the liquids investigated in this work showed deviations from the Arrhenius behaviour at the lower limits of their respective temperature ranges. Therefore, only the ranges in which the data can be well described by eqn (4) are analyzed and shown in Fig. 5.

Fig. 5(b) shows the obtained activation energies E_A for the 1-phenylalkanes and n-alkanes. Additionally, the activation energies are listed in Table 2. For $n \le 8$ the activation energy of the 1-phenylalkanes is only weakly chain length dependent and rather close to the value of toluene (n = 1), while for $n \ge 13$ it follows a trend similar to that of the *n*-alkanes, eventually approaching the latter at n = 19. Furthermore, this strong chain length dependence sets in when the activation energies of the corresponding *n*-alkanes surpass that of toluene (indicated by the grey shaded area).

4. Discussion

The molecules constituting the liquids investigated in this work lack specific electrostatic, dipolar or hydrogen bonding interactions. However, the ring-groups of the molecules are aromatic and therefore π - π interactions between neighbouring rings are likely to occur, while the hydrocarbon tails cannot participate in these interactions. It is therefore likely that a certain degree of nanoscale segregation of rings and chains is the origin of the observed prepeak. However, since the role of π - π interactions in the structuring of aromatic systems is still debated, 36 even in systems where the aromatic ring makes up most of the molecule, we will refrain from assigning the observed structure formation in this work to any specific kind of ordering.

The temperature independence of the prepeak position presented in Fig. 3(a) suggests that there is no growth of the associated characteristic length scale with decreasing temperature, in contrast to the results for imidazolium based ionic liquids.1 Since the 1-phenylalkanes are single component liquids and the units involved in the nanoscale segregation are part of the same molecule, this is not surprising. Regarding the temperature dependence of the prepeak amplitude presented in Fig. 3(b), the temperature independent amplitude for n = 8 and the decreasing amplitude with temperature for $n \ge 13$ indicates that the observed structures are more resistant to inter-diffusion of rings and chains at short alkyl chain lengths and become more dynamic with increasing chain length, as aromatic ring-ring interactions become less important. As shown in Fig. 5(b) this transition is mirrored in the chain length dependence of the activation energy of molecular reorientation. The activation energy is only weakly dependent on the chain length for $n \leq 8$ and close to the value of toluene. For toluene, only a methyl group is attached to the phenyl ring, therefore its rotation should be mainly controlled by ring-ring interactions. As soon as the activation energy of the corresponding n-alkanes surpasses that of toluene, the activation energy of the 1-phenylalkanes starts to follow the chain length dependence of that of the *n*-alkanes. This implies that molecular reorientation at these chain lengths is no longer fully controlled by ring-ring interactions. In total, the role of the phenyl rings in structure formation as well as wholemolecule reorientation is very apparent for $n \le 8$ and diminishes for $n \ge 13$. At the threshold of around n = 8 also the bimodality of the relaxation peak starts to become more pronounced. The latter result in combination with the interpretation of the X-ray scattering curves reveals a rather clear relation between structure and dynamics: Nanoscale segregation of rings and chains leads to regions where rings rotate in the vicinity of other rings. For $n \le 8$ specific regions are rather stable and result in molecular reorientation being controlled by ring-ring interactions. For $n \geq 13$ the structures become more dynamic, resulting in molecular reorientation no longer being controlled by ring-ring interactions and the corresponding activation energy increases similar to that of the corresponding *n*-alkanes. However, since the ring group can rotate around the C-C bond connecting it to the chain, dynamic decoupling occurs.

5. Conclusions

By a combined analysis of results from X-ray scattering and depolarized dynamic light scattering we conclude that both structure and dynamics in liquid 1-phenylalkanes are controlled by an interplay of interactions between ring groups and interactions between alkyl chains, with ring-ring interactions dominating for chain lengths $n \le 8$ and becoming less important for $n \ge 1$ 13 where chain-chain interactions control the behavior. The transition between the two regimes is seen in the behavior of the activation energy of molecular rotation. For $n \leq 8$ the activation energy is virtually chain length independent and close to that of toluene (n = 1), indicating dynamics dominated by ringring interactions. Increasing the chain length beyond n = 13results in an increase in activation energy that mirrors that of the n-alkanes, eventually approaching the activation energy of the corresponding n-alkane at n = 19, indicating a diminishing

influence of ring-ring interactions on molecular reorientation. This transition is mirrored in the temperature and chain length dependence of the observed prepeak in the X-ray scattering curves. Here, for $n \leq 8$ the amplitude of the prepeak is virtually temperature independent, whereas for $n \ge 13$ the amplitude significantly decreases with increasing temperature, indicating a decreasing dominance of ring-ring interactions, consistent with more dynamic ring aggregates. Since phenylalkanes are among the most simple representatives of liquids consisting of aromatic and non-aromatic units we regard this work as a proof of concept to study the relations between structure and dynamics in liquids with competing interactions weaker than Coulombic interactions or H-bonding.

Data availability

The data presented and analyzed in this study are available from: https://doi.org/10.48328/tudatalib-1690.

Conflicts of interest

There are no conflicts to declare.

Acknowledgements

Financial support by the Deutsche Forschungsgemeinschaft under grant no. 1192/3 is gratefully acknowledged. The Novo Nordisk Foundation is gratefully acknowledged for funding RUCSAXS - Roskilde University Interdisciplinary X-ray Scattering Hub - with grant NNF21OC0068491.

References

- 1 A. Triolo, O. Russina, H.-J. Bleif and E. Di Cola, J. Phys. Chem. B, 2007, 111, 4641-4644.
- 2 T. L. Greaves and C. J. Drummond, Chem. Soc. Rev., 2013,
- 3 C. Gainaru, S. Kastner, F. Mayr, P. Lunkenheimer, S. Schildmann, H. J. Weber, W. Hiller, A. Loidl and R. Böhmer, Phys. Rev. Lett., 2011, 107, 118304.
- 4 R. Böhmer, C. Gainaru and R. Richert, Phys. Rep., 2014, 545,
- 5 J. Gabriel, F. Pabst, A. Helbling, T. Böhmer and T. Blochowicz, Phys. Rev. Lett., 2018, 121, 035501.
- 6 K. L. Eliasen, J. Gabriel, T. Blochowicz, C. P. Gainaru, T. E. Christensen and K. Niss, J. Chem. Phys., 2024, 161, 034506.
- 7 F. Pabst, J. Gabriel and T. Blochowicz, J. Phys. Chem. Lett., 2019, 10, 2130-2134.
- 8 S. Arrese-Igor, A. Alegra, A. Arbe and J. Colmenero, J. Mol. Liq., 2020, 312, 113441.
- 9 S. Ge, S. Samanta, M. Tress, B. Li, K. Xing, P. Dieudonné-George, A.-C. Genix, P.-F. Cao, M. Dadmun and A. P. Sokolov, Macromolecules, 2021, 54, 4246-4256.

- 10 M. Becher, E. Steinrücken and M. Vogel, J. Chem. Phys., 2019, 151, 194503.
- 11 R. Zeißler, F. Pabst, T. Böhmer and T. Blochowicz, Phys. Chem. Chem. Phys., 2023, 25, 16380-16388.
- 12 L. Gontrani, P. Ballirano, F. Leonelli and R. Caminiti, The Structure of Ionic Liquids, Springer, 2013, pp. 1–37.
- 13 Y.-L. Wang, B. Li, S. Sarman, F. Mocci, Z.-Y. Lu, J. Yuan, A. Laaksonen and M. D. Fayer, Chem. Rev., 2020, 120, 5798-5877.
- 14 R. Hayes, G. G. Warr and R. Atkin, Chem. Rev., 2015, 115, 6357-6426.
- 15 O. Russina, B. Fazio, G. Di Marco, R. Caminiti and A. Triolo, The structure of ionic liquids, Springer, 2013, pp. 39-61.
- 16 M. Pozar, J. Bolle, C. Sternemann and A. Perera, J. Phys. Chem. B, 2020, 124, 8358-8371.
- 17 M. Tomsic, A. Jamnik, G. Fritz-Popovski, O. Glatter and L. Vlcek, J. Phys. Chem. B, 2007, 111, 1738-1751.
- 18 N. Franks, M. Abraham and W. Lieb, J. Pharm. Sci., 1993, 82, 466-470.
- 19 M. J. Servis, M. Piechowicz, I. A. Shkrob, L. Soderholm and A. E. Clark, *J. Phys. Chem. B*, 2020, **124**, 10822–10831.
- 20 T. Rahman, B. L. Bonnett, D. Poe, P. N. Wimalasiri, S. Seifert, J. Lal, G. B. Stephenson and M. J. Servis, J. Mol. Liq., 2024, 393, 123625.
- 21 G. G. Warr and R. Atkin, Curr. Opin. Colloid Interface Sci., 2020, 45, 83-96.
- 22 X. Zhang, K. Kyriakos, M. Rikkou-Kalourkoti, E. N. Kitiri, C. S. Patrickios and C. M. Papadakis, Colloid Polym. Sci., 2016, 294, 1027-1036.
- 23 A. Triolo, V. V. Chaban, F. L. Celso, F. Leonelli, M. Vogel, E. Steinrücken, A. Del Giudice, C. Ottaviani, J. A. Kenar and O. Russina, J. Mol. Liq., 2023, 369, 120854.
- 24 B. J. Berne and R. Pecora, Dynamic light scattering: with applications to chemistry, biology, and physics, Courier Corporation, 2000.
- 25 J. Gabriel, F. Pabst, A. Helbling, T. Böhmer and T. Blochowicz, The Scaling of Relaxation Processes, Springer, 2018, pp. 203-245.
- 26 T. Böhmer, F. Pabst, J. Gabriel, R. Zeißler and T. Blochowicz, arXiv, 2024, preprint, arXiv:2412.17014.
- 27 P. Lunkenheimer, U. Schneider, R. Brand and A. Loid, Contemp. Phys., 2000, 41, 15-36.
- 28 H. V. Annapureddy, H. K. Kashyap, P. M. De Biase and C. J. Margulis, J. Phys. Chem. B, 2010, 114, 16838-16846.
- 29 S. Schramm, T. Blochowicz, E. Gouirand, R. Wipf, B. Stühn and Y. Chushkin, J. Chem. Phys., 2010, 132, 224505.
- 30 W. W. Graessley, Macromolecules, 2002, 35, 3184-3188.
- 31 L. L. Thomas, T. J. Christakis and W. L. Jorgensen, J. Phys. Chem. B, 2006, 110, 21198-21204.
- 32 K. Fujii, S. Kohara and Y. Umebayashi, Phys. Chem. Chem. Phys., 2015, 17, 17838-17843.
- 33 E. A. Rössler and M. Becher, J. Chem. Phys., 2024, 160, 074501.
- 34 A. Schönhals and F. Kremer, Broadband dielectric spectroscopy, Springer, 2003, pp. 59-98.
- 35 B. Schmidtke, N. Petzold, R. Kahlau, M. Hofmann and E. Rössler, Phys. Rev. E, 2012, 86, 041507.
- 36 C. R. Martinez and B. L. Iverson, Chem. Sci., 2012, 3, 2191-2201.